patients only once a week, whereas a standard IFN without pegylation used to be injected up to three to five times a week. This once-a-week injection of pegylated IFNs in combination with daily oral dosing of the nucleoside analogue ribavirin has substantially improved the rate of sustained virological response in patients with chronic HCV infection and got a position as the first line therapy [8,9]. We previously reported that PEG-IFN-α2b which contains 12 kDa polyethylene glycol (PEG) has stronger antitumor effects *in vivo* than non-pegylated IFNs and this result might be indicating that continuous IFNs exposure to cancer cells in body is more effective than continual injection [10]. On the basis of above-described background, we examined the growth inhibitory effects of PEG-IFN-α2a which contains two chains of 20 kDa PEG and has the longest serum half-life among clinically available IFNs on liver cancer cell lines *in vitro* and *in vivo*.

Methods

Cell Lines and Cell Culture

This study used 11 HCC cell lines (KIM-1, KYN-1, KYN-2, KYN-3, HAK-1A, HAK-1B, HAK-2, HAK-3, HAK-4, HAK-5, and HAK-6) and 2 human combined hepatocellular and cholangiocarcinoma (CHC) cell lines (KMCH-1 and KMCH-2). These HCC and CHC cell lines were originally established in our laboratory, and each cell line retains the morphological and functional features of the original tumor as described elsewhere [11–20]. Since tumorigenicity is higher in HAK-1B and KIM-1 cells than in the other 11 cell lines that we have, we used these two cell lines for *in vivo* study.

The cells were grown in Dulbecco's Modified Eagle Medium (Nissui Seiyaku, Co., Japan) supplemented with 2.5% heat-inactivated (56°C, 30 min) fetal bovine serum (FBS, Bioserum, Victoria, Australia), 100 U/mL penicillin, 100 μg/mL streptomycin (GIBCO BRL/Life Technologies, Inc., Gaithersburg, MD) and 12 mmol/L sodium bicarbonate, in a humidified atmosphere of 5% CO_2 in air at 37°C.

IFN and Reagents

PEG-IFN-α2a (PEGASYS®, Chugai Pharmaceutical Co., Ltd., Tokyo, Japan) with the specific activity of 1.4 X 10^7 IU/mg protein and non-pegylated IFN-α2a (Miltenyi Biotec GmbH, Bergisch Gladbach, Germany) with that of 2.0 X 10^8 IU/mg protein were used in the study.

Anti-bromodeoxyuridine (BrdU) antibody and fluorescein isothiocyanate-conjugated goat anti-mouse immunoglobulin (FITC-GAM) were purchased from Becton Dickinson Immunocytometry Systems USA (San Jose, CA); control normal mouse IgG_1, from DAKO (Glostrup, Denmark); rat antibody against mouse endothelial cells (anti-CD34, clone MEC14.7), from Serotec Co., UK; and mouse monoclonal antibody against human α-smooth muscle actin (SMA) that cross-reacts with mouse α-SMA (clone 1A4).

Effects of PEG-IFN-α2a on the Proliferation of HCC and CHC Cell Lines *in vitro*

The effects of PEG-IFN-α2a on the growth of the cultured cells were examined with colorimetry using 3-(4,5-dimethylthiazol-2yl)-2,5-diphenyl tetrazolium bromide (MTT) assay kits (Chemicon, Temecula, CA) as described elsewhere [18,21]. Briefly, the cells (1.5~8 X 10^3 cells per well) were seeded on 96-well plates (Nunc, Inc, Roskilde, Denmark), cultured for 24 hours, and the culture medium was changed to a new medium with or without PEG-IFN-α2a (0.016, 0.064, 0.256, 1.024, 4.096, 16.4, 65.5, 262, 1,048, or 4,194 ng/mL). After culturing for 24, 48, 72 or 96 hours, the number of viable cells was measured with ImmunoMini NJ-2300 (Nalge Nunc International, Tokyo, Japan) by setting the test wavelength at 570 nm and the reference wavelength at 630 nm. To keep the optical density within linear range, all experiments were performed while the cells were in the logarithmic growth phase.

Quantitative analysis of apoptotic cells induced by PEG-IFN-α2a

HAK-1B or KIM-1 cells cultured with medium alone (control), non-pegylated IFN-α2a (10 ng/ml=2,000 IU/ml) or PEG-IFN-α2a (144 ng/ml=2,000 IU/ml) for 72 hours were stained with the Annexin V-EGFP (enhanced green fluorescent protein) Apoptosis Detection Kits (Medical & Biological Laboratories Co., Ltd.) according to the manufacturer's instructions. After staining, the cells were analyzed using a FACScan (Becton Dickinson Immunocytometry Systems, San Jose, CA), and Annexin V-EGFP-positive apoptotic cell rate was determined.

Morphological Observation

For morphological observation under a light microscope, cultured cells were seeded on Lab-Tek tissue culture chamber slides (Nunc, Inc.), cultured with or without PEG-IFN-α2a (262, 1,048 or 4,194 ng/mL) for 72 hours, fixed for 10 min in Carnoy's solution, and stained with hematoxylin-eosine (HE).

Effects of PEG-IFN-α2a on HCC Cell Proliferation in Nude Mice

All animal experiments were approved by the institutional committee for animal experiments in Kurume University School of Medicine (Permit Number: 1334), and conducted according to the Guide for the Care and Use of Laboratory Animals of the National Institute of Health and the Regulations for Animal Experimentation of Kurume University School of Medicine. Mice were killed by cervical dislocation under diethyl ether anesthesia, and all efforts were made to minimize suffering. Cultured HAK-1B or KIM-1 (10^7 cells/mouse) was subcutaneously (s.c.) injected into the backs of 5-week-old female BALB/c athymic nude mice (Clea Japan, Inc., Osaka, Japan). Five to seven days later when the largest diameter of the tumor, which was measured by using caliper, reached approximately 5~10 mm (Day 0), tumor volume (mm^3) was calculated in the equation 'the largest diameter X (the smallest diameter)^2 X 0.5', and then the mice were divided into 5 groups (n=8 each). Tumor volume was measured on Day 0, 1, 2, 4, 6, 8, 10, 12, and 14. Mouse body weight was measured on Day 0,

8, and 14. After 2-week treatment, mice were killed on Day 15 and the actual tumor weight was also measured. In experiment 1, the 5 groups of 8 mice received either phosphate-buffered saline (PBS) (Control) or PBS with the different dosages of PEG-IFN-α2a (0.06–60 μg) once a week for 2 consecutive weeks (Day 1 and Day 8). The clinical dose of PEG-IFN-α2a in chronic hepatitis C treatment is about 3 μg/kg and is equivalent to the lowest dose (0.06 μg/mouse=840 IU/mouse) in this experiment. After killing, resected tumors were used for morphological studies (e.g., HE staining and immunohistochemistry) and Enzyme-linked immunosorbent assay (ELISA) analysis. Every mouse received an intraperitoneal injection of 1 mg of BrdU 30 min before killing. In experiment 2, to examine the difference between non-pegylated and pegylated IFNs, 5 groups of 8 mice received either PBS (Control), PBS with 0.0042 or 0.042 μg of IFN-α2a (840 or 8,400 IU, respectively), or PBS with 0.06 or 0.6 μg of PEG-IFN-α2a (840 or 8,400 IU, respectively). In this experiment, tumor weights on Day 15 and numbers of apoptotic cells were compared among the groups.

Morphological Examination of the Subcutaneous Tumors of Nude Mice

The number of cells showing the characteristics of apoptosis (e.g., cytoplasmic shrinkage, chromatin condensation, and nuclear fragmentation) was counted in at least three 0.25 mm^2-areas within an HE-stained specimen, and the average number per area was obtained. The TUNEL technique (ApopTag® Peroxidase *In Situ* apoptosis Detection Kits, CHEMICON International, Inc, CA) was used to detect apoptotic cells, and the average number of TUNEL-positive cells per area was obtained, as described above. The specimens were also immunostained for incorporated BrdU using BrdU Staining Kits (Oncogene Research Products, Boston, MA), and the average number of positive cells per area was obtained as described above. In addition, double-immunostaining was performed with anti-mouse endothelial cell antibody, anti-human α-SMA antibody, Histofine simple stain mouse MAX-PO (Rat) kits (Nichirei, Tokyo, Japan), and HistoMouse™-plus kits to detect artery-like blood vessels as described in our previous report [21,22]. The number of double-immunostaining-positive blood vessels in the tumor was counted on each specimen. Granulation tissue within the tumor were excluded in counting of blood vessels. The size of the counted area was measured by tracing the outline displayed on a computer monitor using Mac SCOPE (MITANI Corp., Chiba, Japan). From the obtained number of vessels per unit area (mm^2), the group mean was obtained for group comparison.

Enzyme-linked immunosorbent assay (ELISA)

Portions of the resected xenograft tumors were homogenized in 500 μl of ice-cold Ca^{2+} and Mg^{2+}-free PBS containing 100 mg/ml phenymethylsulfonyl fluoride using a pellet pestle. The mixture was centrifuged for 10 min (12,000 g, 4°C), and the supernatant was stored at -20°C until use. After the determination of the amount of the tissue protein in the supernatant using a BCA protein assay reagent (Pierce, Rockford, IL), the amount of basic fibroblast growth factor (bFGF) and IL-8 was measured by using commercially available ELISA kits (R&D Systems, Minneapolis, MN).

Statistics

Comparisons of estimated tumor volume and colorimetric cell growth were performed using two-factor factorial ANOVA and Student's *t*-test, respectively. The other data comparisons were performed using the Mann-Whitney U test.

Results

Effects of PEG-IFN-α2a on Liver Cancer Cell Proliferation *in vitro*

Twenty-four hours after the addition of 4,194 ng/mL of PEG-IFN-α2a, mild increase in the relative viable cell number occurred in 9 cell lines (all cell lines except KYN-2, HAK-1A, HAK-6, and KMCH-1). However, after 72 hours or later, a 10% or more decrease in the cell number occurred in all cell lines (Figure 1A). In HAK-2, HAK-3, and HAK-4, HAK-6, and KMCH-2, proliferation was suppressed up to 72 hours and the cell number reached a plateau or slightly increased thereafter. In the other 8 cell lines, proliferation was suppressed to varying degrees up to 96 hours.

The relative viable cell number was suppressed in 11 cell lines (all cell lines except HAK-1A and KMCH-2) in a dose-dependent manner after the 96 hours-incubation with PEG-IFN-α2a (Figure 1B). In 7 cell lines (HAK-1B, KMCH-1, KIM-1, KYN-1, HAK-6, KYN-3, and KYN-2), the number was suppressed to 50% or less with 4,194 ng/mL of PEG-IFN-α2a, and the 50% inhibitory concentration (IC50) was 253 ng/mL for HAK-1B, 670 ng/mL for KMCH-1, 1,105 ng/mL for KIM-1, 1,128 ng/mL for KYN-1, 1,302 ng/mL for HAK-6, 1,524 ng/mL for KYN-3, and 4,431 ng/mL for KYN-2. No relationship was detected between the histological differentiation level of the original tumor and sensitivity to the anti-proliferative effect of PEG-IFN-α2a.

Seventy-two hours after adding 4,194 ng/mL of PEG-IFN-α2a, 8 cell lines (all cell lines except KYN-3, HAK-1A, HAK-2, HAK-3, and KMCH-2) showed characteristics of apoptosis, e.g., cytoplasmic shrinkage, chromatin condensation, and nuclear fragmentation, in various degrees and in a dose-dependent manner (Figure 2). The appearance of apoptosis was further confirmed in HAK-1B and KIM-1 cells cultured with 10 ng/ml (=2,000 IU/ml) of IFN-α2a or 144 ng/ml (=2,000 IU/ml) of PEG-IFN-α2a by apoptosis detection assay (Table 1). Non-pegylated IFN-α2a induced much more apoptosis than PEG-IFN-α2a.

Effects of PEG-IFN-α2a on HCC Cell Proliferation in Nude Mice

Chronological changes in estimated tumor volume after subcutaneous injection of cultured HAK-1B or KIM-1cells to nude mice are summarized in Figure 3. Dose-dependent suppression of tumor volume was observed in mice receiving PEG-IFN-α2a. In the experiment of HAK-1B tumors, a significant difference in the changes in tumor volume and tumor weight was observed between the Control mice and the mice

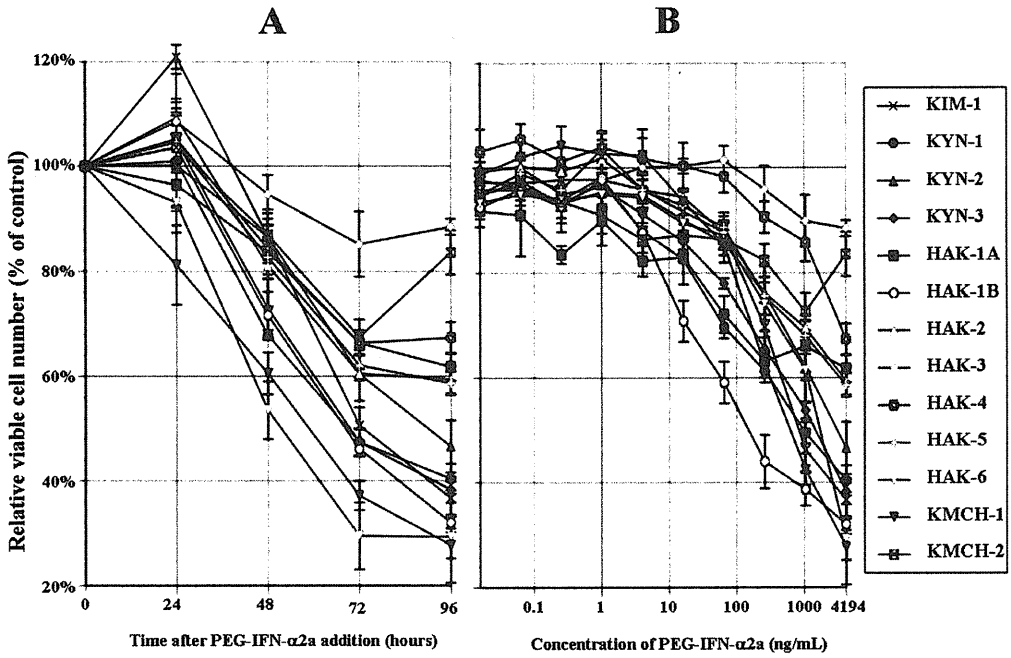

Figure 1. Anti-proliferative effect of PEG-IFN-α2a. (A) Chronological changes in relative viable cell number (% of the control) after adding 4,194 ng/mL of PEG-IFN-α2a. Growth was suppressed with time in 8 cell lines. (B) 96 hours after adding 10 different concentrations of PEG-IFN-α2a. Cell proliferation was suppressed in a dose-dependent manner in 11 cell lines. The suppression was significant ($P < 0.0001$~0.05) in the ranges of 0.016~4,194 ng/mL of PEG-IFN-α2a in HAK-6, 0.256~4,194 ng/mL in KYN-3 and HAK-1A, 4.096~4,194 ng/mL in KIM-1, KYN-1, HAK-1B, HAK-2 and KMCH-2, 16.4~4,194 ng/mL in KYN-2, HAK-5 and KMCH-1, 262~4,194 ng/mL in HAK-4, and at 4,194 ng/mL in HAK-3 (Student *t*-test). Eight samples were used in each experiment (n = 8). The experiment was repeated at least 3 times for each cell line. The figures represent average ± SE of the experiments.

doi: 10.1371/journal.pone.0083195.g001

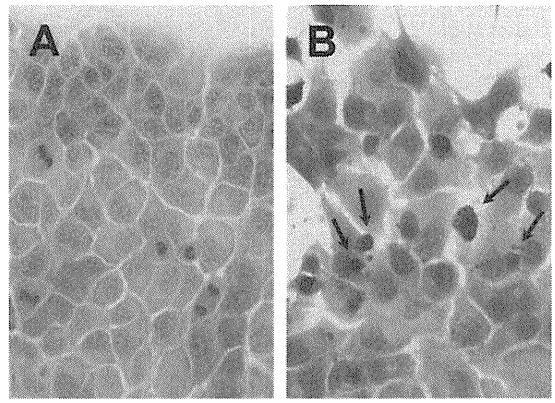

Figure 2. Photomicrograph of HAK-1B cells cultured for 72 hours on a Lab-Tek Chamber slide. (A) Without PEG-IFN-α2a in culture medium. (B) With 4,194 ng/mL of PEG-IFN-α2a in culture medium. Apoptotic cells (short arrows) characterized by cytoplasmic shrinkage, chromatic condensation and nuclear fragmentation were noted (HE staining, X 200).

doi: 10.1371/journal.pone.0083195.g002

Table 1. Quantitative analysis of apoptosis in HAK-1B or KIM-1.

	Annexin V-EGFP apoptotic cells (%)		
Cell line[a]	Control	IFN-α2a	PEG-IFN-α2a
HAK-1B	4.1 ± 0.5[b]	18.5 ± 0.3	10.9 ± 0.5
KIM-1	9.4 ± 0.4	47.0 ± 0.2	29.8 ± 2.1

[a] Cells were cultured with medium alone (Control), IFN-α2a (10 ng/ml=2,000 IU/ml) or PEG-IFN-α2a (144 ng/ml=2,000 IU/ml). [b] Mean ±SE.

doi: 10.1371/journal.pone.0083195.t001

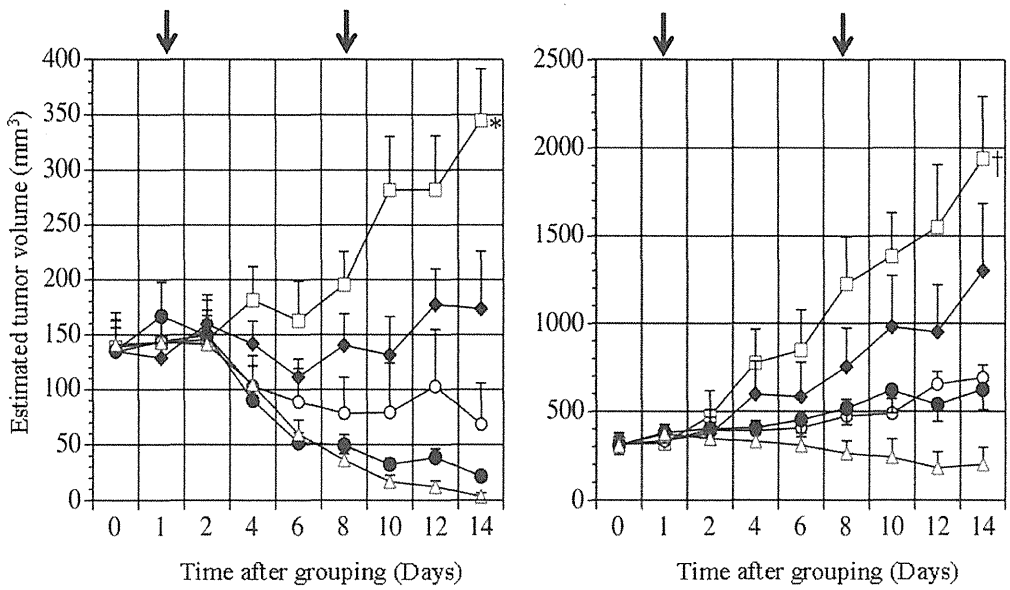

Figure 3. Time-course change in estimated tumor volumes of subcutaneously transplanted HAK-1B (A) or KIM-1 (B) tumors in nude mice in Experiment 1. The mice received a subcutaneous injection of 0.06 (▲), 0.6 (○), 6 (●), or 60 (△) μg of PEG-IFN-α2a, or medium alone (Control) (□), once a week for 2 consecutive weeks. The arrows show the days of injection. The figures represent average ± SE. *P < 0.0001, versus the other groups. †P < 0.01, versus the other groups.

doi: 10.1371/journal.pone.0083195.g003

that received 0.06, 0.6, 6 or 60 μg of PEG-IFN-α2a (P < 0.0001 by two-factor factorial ANOVA; and P < 0.001~0.02 by the Mann-Whitney U test, Figure 3A and Table 2). In the experiment of KIM-1 tumors, a significant reduction of tumor volume was also observed with the use of PEG-IFN-α2a (P < 0.001 by two-factor factorial ANOVA, Figure 3B). There were significant differences in the actual tumor weight between the Control group and the PEG-IFN-α2a groups, except for the PEG-IFN-α2a (0.06 μg) group (Table 2). The actual tumor weight at the end of the experiment 2 was summarized in Table 3. Subcutaneous injection of 0.6 μg of PEG-IFN-α2a induced the significant reduction of tumor weight, compared with the Control group and the group that received the same international unit of non-pegylated IFN-α2a (P<0.005 and P<0.03, respectively). In this experiment, there was no significant difference between the Control group and the PEG-IFN-α2a (0.06 μg) group (P=0.078).

Histological examination of the HAK-1B tumor specimens stained with HE revealed that the numbers of apoptotic cells in the mice treated with PEG-IFN-α2a (0.06 or 0.6 μg) were significantly higher than that of the Control, and the number increased dose dependently (Figure 4, A and B; Table 4). The incidence of apoptosis in TUNEL-stained sections showed the same tendencies as those obtained in HE-stained sections (Figure 4C and Table 4). Immunohistochemical examination of BrdU uptake in HAK-1B tumors revealed that there was no significant difference in BrdU labeling index between the Control and PEG-IFN-α2a (0.06 or 0.6 μg) groups (Table 4). As for apoptosis, similar findings were observed in experiment 2 in which KIM-1 was used. The group treated with 0.6 μg of PEG-IFN-α2a showed increased number of apoptotic cells than the control group. There was no significant difference between the control and IFN-α2a group. In addition, the group treated with

Table 2. The weight of subcutaneous tumors of HAK-1B or KIM-1 cells in nude mice at killing (Experiment 1).

	Tumor weight (g)	
Treatment group[a]	HAK-1B	KIM-1
Control	0.303 ± 0.05[b, c]	1.050 ± 0.24[e]
PEG-IFN-α2a (0.06 μg)	0.141 ± 0.03[d]	0.725 ± 0.17[f]
PEG-IFN-α2a (0.6 μg)	0.033 ± 0.01	0.439 ± 0.04
PEG-IFN-α2a (6 μg)	0.015 ± 0.01	0.434 ± 0.04
PEG-IFN-α2a (60 μg)	0.0	0.076 ± 0.05

[a] Cultured HAK-1B or KIM-1 cells (1.0 X 10^7) were subcutaneously transplanted into nude mice. Five groups of 8 mice received either phosphate-buffered saline (PBS) (Control) or PBS with the different dosages of PEG-IFN-α2a (0.06–60 μg) once a week. All mice were killed and the tumor weight was measured on the 15th day. [b] Mean ± SE. [c] $P < 0.02$, versus the PEG-IFN-α2a (0.06 μg) group; $P < 0.001$, versus the PEG-IFN-α2a (0.6 μg) group; $P < 0.001$, versus the PEG-IFN-α2a (6 μg) group. [d] $P < 0.02$, versus PEG-IFN-α2a (60 μg). [e] Not significant, versus the PEG-IFN-α2a (0.06 μg) group; $P < 0.03$, versus the PEG-IFN-α2a (0.6 μg) group; $P < 0.05$, versus the PEG-IFN-α2a (6 μg) group; $P < 0.01$, versus the PEG-IFN-α2a (60 μg) group. [f] $P < 0.05$, versus the PEG-IFN-α2a (60 μg) group.

doi: 10.1371/journal.pone.0083195.t002

Table 3. The actual weight and numbers of apoptotic cells of subcutaneous tumors at killing (Experiment 2).

Treatment group[a]	activity of interferon (IU)	Tumor weight (g)	Apoptosis (Number of cells/0.25mm^2)
Control	0 IU	0.726 ± 0.09[b, c]	7.6 ± 0.9[d]
IFN-α2a (0.0042 μg)	840 IU	0.588 ± 0.07[d]	7.9 ± 0.9[g]
IFN-α2a (0.042 μg)	8,400 IU	0.531 ± 0.04[e]	7.6 ± 0.7[h]
PEG-IFN-α2a (0.06 μg)	840 IU	0.493 ± 0.04[f]	8.9 ± 0.9
PEG-IFN-α2a (0.6 μg)	8,400 IU	0.355 ± 0.03	9.7 ± 1.0*

[a] Cultured HAK-1B cells (1.0 X 10^7) were subcutaneously transplanted into nude mice. Five groups of 8 mice received either PBS (Control), PBS with 0.0042 or 0.042 μg of IFN-α2a (840 or 8,400 IU, respectively), or PBS with 0.06 or 0.6 μg of PEG-IFN-α2a (840 or 8,400 IU, respectively). All mice were killed and the tumor weight was measured on the 15th day. The number of apoptotic cells was counted in at least three 0.25 mm^2-areas in each section stained with hematoxylin and eosin, and the average number per area in each group was obtained. [b] Mean ± SE. [c] $P < 0.005$, versus the PEG-IFN-α2a (0.6 μg) group. [d] $P < 0.02$, versus the PEG-IFN-α2a (0.6 μg) group. [e] $P < 0.03$, versus the PEG-IFN-α2a (0.6 μg) group. [f] $P < 0.02$, versus the PEG-IFN-α2a (0.6 μg) group. [g] $P < 0.05$, versus the PEG-IFN-α2a (0.6 μg) group. [h] $P < 0.001$, versus the PEG-IFN-α2a (0.6 μg) group.

doi: 10.1371/journal.pone.0083195.t003

0.6 μg of PEG-IFN-α2a (8,400 IU) showed higher number of apoptotic cells than those with 0.042 μg of IFN-α2a (8,400 IU).

The resected tumor of the PEG-IFN-α2a group showed granulation tissue at the middle of the tumor to various degrees (Figure 5). Arteries that appeared in the granulation tissue were excluded in blood vessel count within tumor. There was no significant difference in the number of blood vessels per unit area within the HAK-1B tumor and the expression of bFGF and IL-8 in the tumors between the PEG-IFN-α2a group and the Control group (Figure 5; Table 5).

Discussion

In the *in vitro* study, we showed that PEG-IFN-α2a inhibit the growth of 8 and 11 out of 13 cell lines in a time- and dose-dependent manner, however, PEG-IFN-α2a was apparently less active on an IC50 basis, compared with either PEG-IFN-α2b or IFN-α2b or consensus IFN-α or BALL-1 lymphoblastoid IFN-α which was tested in the same experimental condition in our previous reports [10,18,21]. For example, IC50 for HAK-1B cells was approximately 253 ng/ml of PEG-IFN-α2a, 13.1 ng/ml of PEG-IFN-α2b, 2.4 ng/ml of IFN-α2b, 0.7 ng/ml of consensus IFN-α and 1.1 ng/ml of BALL-1 lymphoblastoid IFN-α. On the other hand, in the *in vivo* study, s.c. injection of PEG-IFN-α2a once a week showed better antitumor effect on a tumor volume or weight basis, compared with that of non-pegylated IFN-α2a. These results might support our hypothesis that continuous contact with IFNs induces strong *in vivo* antitumor effects, and are not surprising because it was reported that PEG-IFN-α2a showed less active in vitro antiviral activity and but had much more *in vivo* antitumor activity than non-pegylated IFN-α2a [23]. We also showed that PEG-IFN-α2a can inhibit the proliferation of CHC cell lines as well as HCC. In MTT assay, the growth of KMCH-1 was well suppressed although another CHC cell line, KMCH-2 was not. One possible explanation for the different sensitivity between KMCH-1 and KMCH-2 is that the origin of KMCH-1 is CHC, classical type and that of KMCH-2 is CHC with stem-cell features, intermediate-cell subtype according to the latest WHO classification [24]. Such a stem-cell properties of the tumor might be the reason for IFN resistance. Another interesting finding in the *in vitro* study is the discrepancy between the results of MTT assay and apoptosis detection assay. When HAK-1B or KIM-1 was cultured with PEG-IFN-α2a, IC50 for HAK-1B was much lower than that for KIM-1 although HAK-1B showed lower rate of apoptotic cells than KIM-1. These findings suggest that there might be some

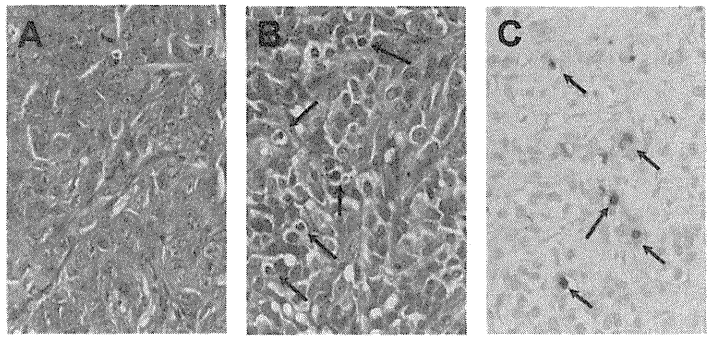

Figure 4. Photomicrograph of subcutaneous human HCC tumor in nude mice that was developed after the injection of HAK-1B cells. (A) A control mouse that received culture medium alone. The tumor shows a compact arrangement of tumor cells and a sinusoid-like structure in the stroma. (B) A mouse that received a s.c. injection of 0.06 μg of PEG-IFN-α2a. There are some apoptotic tumor-cells characterized by shrinkage and eosinophilic change in the cytoplasm, chromatin condensation and/or fragmentation of nuclei (arrows, HE staining, X200). (C) The same tumor as shown in (B). There are some TUNEL-positive cells showing brown nuclei (arrows, stained by the TUNEL technique, X200).

doi: 10.1371/journal.pone.0083195.g004

Table 4. Numbers of apoptotic cells and BrdU-positive cells in human HCC tumors subcutaneously transplanted in nude mice.

	Apoptosis[b] (Number of cells/0.25mm^2)		BrdU Labeling Index[c] (Number of positive cells/0.25mm^2)
Treatment group[a]	HE stain	TUNEL method	
Control	8.4 ± 0.8[d,e]	9.6 ± 1.1[e]	32.3 ± 1.6[f]
PEG-IFN-α2a (0.06 μg)	12.2 ± 1.0	15.4 ± 1.8	27.0 ± 2.6
PEG-IFN-α2a (0.6 μg)	12.4 ± 0.9	16.1 ± 1.5	31.3 ± 6.9

[a] Cultured HAK-1B cells (1.0 X 10^7) were subcutaneously transplanted into nude mice. Five groups of 8 mice received either phosphate-buffered saline (PBS) (Control) or PBS with the different dosages of PEG-IFN-α2a (0.06–60 μg) once a week. Tumors of mice that received 6 or 60 μg of PEG-IFN-α2a could not be used because the tumors were too small to evaluate. All mice were killed on the 15th day. [b] The number of apoptotic cells was counted in at least three 0.25 mm^2-areas in each section stained with hematoxylin and eosin, and the average number per area in each group was obtained. The number of TUNEL-positive cells was also counted in the same manner. [c] The number of BrdU-positive cells was counted in at least three 0.25 mm^2-areas in each section, and the average number per area in each group was obtained as the labeling index. [d] Mean ± SE. [e] $P < 0.02$, versus the other groups. [f]. Not significant, versus the other groups.

doi: 10.1371/journal.pone.0083195.t004

mechanisms other than apoptosis, which affect the sensitivity to antitumor effects of PEG-IFN-α2a. We previously reported that both pegylated and non-pegylated IFN-α inhibited the proliferation of cultured HCC cells by inducing the cell-cycle arrest [10,18]. The expression of interferon receptor on tumor cells might be a possible factor related to antitumor effect. For instance, Nagano et al reported that the expression of this type I IFN receptor on HCC tissue might be a useful predictor to find potential responder to INF-α/5-fluorouracil combination therapy [25]. Immunomodulation by IFNs has also been well studied as a factor related to antitumor effect. In this study, we used athymic mice, which lack mature T-cell, and human IFNs. Since IFNs are species-specific [26], we surmise that this immunomodulatory effect is limited in our study, but this should be confirmed in the future study using mouse IFN.

Morphological observation of the subcutaneous tumors of nude mice revealed that s.c. injection of PEG-IFN-α2a induce the significant increase of apoptotic cells compared with Control group. This result in the *in vivo* study is consistent with that in the *in vitro* study showing characteristic changes of apoptosis after adding PEG-IFN-α2a. Although the inhibition of angiogenesis as well as the induction of apoptosis is regarded as one of the biological effects of IFNs, there was no significant difference in the number of artery-like blood vessels of the subcutaneous tumors between the control and treatment groups. There are two possible explanations of this finding. Firstly, PEG-IFN-α2a was less effective for mouse endothelial cells compared with human cancer cells due to the species specificity of human IFNs. Secondly, it might be difficult to visualize the alteration in the number of vessels in order to examine the efficacy of drugs that possess antiangiogenic

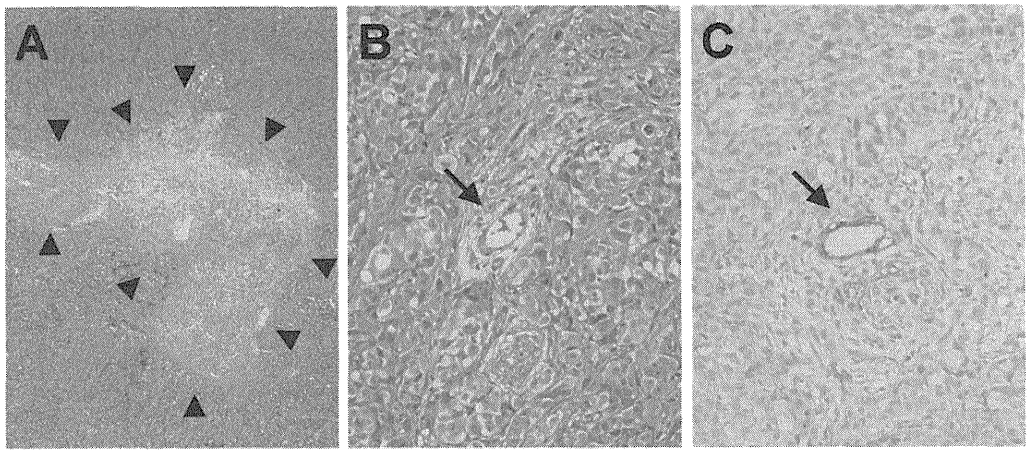

Figure 5. Photomicrograph of resected HAK-1B tumor. (A) Tumor cells are replaced with large granulation tissue at the middle of resected tumor. (arrowheads, HE staining, X20). (B) Artery-like blood vessels in the tumor (arrow, HE staining, X200). (C) Artery-like blood vessel in the tumor (arrow, CD34/α-SMA double-immunostain, X200).

doi: 10.1371/journal.pone.0083195.g005

Table 5. Numbers of artery-like blood vessels, and Enzyme-linked immunosorbent assay (ELISA) of angiogenesis factors in human HCC tumors subcutaneously transplanted in nude mice.

	Artery-like blood vessel[b] (Number of vessels/mm2)	Levels in the tumor lysate[c] (pg/40 μg cellular protein)	
Treatment group[a]	Inside of tumor	bFGF	IL-8
Control	0.104 ± 0.02[d,e]	14.0 ± 1.8[e]	2.8 ± 1.0[e]
PEG-IFN-α2a (0.06 μg)	0.194 ± 0.05	19.8 ± 2.1	4.9 ± 1.3

[a] Cultured HAK-1B cells (1.0 X 10^7) were subcutaneously transplanted into nude mice. Five groups of 8 mice received either phosphate-buffered saline (PBS) (Control) or PBS with the different dosages of PEG-IFN-α2a (0.06–60 μg) once a week. Tumors of mice that received 0.6, 6 or 60 μg of PEG-IFN-α2a could not be used because the tumors were too small to evaluate. All mice were killed on the 15th day. [b] The number of artery-like blood vessels within tumor was counted on each section, and the average number per area in each group was obtained. [c] The expression levels of basic fibroblast growth factor (bFGF) and IL-8 of the resected tumors were measured by ELISA. [d] Mean ± SE. [e]. Not significant, versus the PEG-IFN-α2a (0.06 μg) group.

doi: 10.1371/journal.pone.0083195.t005

activity. Hlatky et al explained in their review article that the reason is that the tightness of the coupling between vessel drop-out and tumor-cell drop-out after the treatment is different [27]. We had observed similar findings in our previous report in which human HCC tumors subcutaneously transplanted in nude mice showed much apoptosis in either PEG-IFN-α2b or IFN-α2b treatment group compared with the Control group, but no significant difference in the number of blood vessels [10]. Kojiro et al also showed that s.c. injection of BALL-1 lymphoblastoid IFN-α increase the number of artery-like blood vessels and the protein expression of bFGF within HCC xenograft tumors in spite of the significant decrease of actual tumor weight [28]. In contrast, Dinney et al showed that IFN-α2a decreases the blood vessel density and the expression of bFGF in orthotopic xenograft model of bladder tumor [29]. The reason for these contrary findings remains unclear and further evaluation with caution is needed by using different doses and types of IFNs and different cell lines, not only in subcutaneous tumor model but also in orthotopic model.

The association between IFN therapy and occurrence or recurrence of HCC has been investigated in some reports. HALT-C trial group showed in their randomized control trial in a large cohort that long-term PEG-IFN-α2a therapy does not reduce the incidence of HCC among patients with chronic HCV infection who have previously failed to achieve a sustained virologic response to therapy [30]. Among only patients with cirrhosis, long-term PEG-IFN-α2a therapy reduced a risk of HCC after a long-time observation [31]. EPIC study group also showed long-term PEG-IFN-α2b therapy does not prevent HCC [32]. On the other hand, Nishiguchi et al reported that long-term IFN-α therapy after curative resection of HCV-related HCC prolongs the survival rate, although preventive effect of intrahepatic recurrence was marginal [33]. Sakaguchi et al also showed that among patients who underwent radical

radiofrequency therapy for HCV-related HCC, long-term IFN-α2b therapy reduced the recurrent rate of HCC [4]. These reports with conflicting results may be suggesting that IFN therapy is effective only after the initial curative treatment of HCV-related HCC. In addition, there are several reports that support that IFN therapy prevents the development of HCC among patients with chronic HBV infection or those underwent curative resection of HBV-related HCC [5,7]. Thus the chemopreventive effect of IFNs against HCC are still controversial, and mechanisms behind that remain unclear. Antiviral effect against HBV and HCV, which are risk factors for HCC, and immunomodulatory effect of IFNs are regarded as main mechanisms. Another possible mechanism is that IFNs may suppress the growth of clinically undetectable HCC due to their direct antitumor effect. Our finding in the current study provide the evidence that PEG-IFN-α2a possesses the direct antitumor effect against HCC.

In conclusion, we demonstrated antitumor effect of PEG-IFN-α2a for human liver cancer cells *in vitro* and *in vivo* and our results suggest that longer contact to IFNs may induce stronger antitumor effect in body. PEG-IFN-α2a might be a possible treatment option for HCC as well as chronic viral hepatitis. Further studies are needed from both molecular and clinical view points in order to find out particular patient group those respond to this therapy.

Acknowledgements

We thank Ms. Akemi Fujiyoshi for her assistance in our experiments.

Author Contributions

Conceived and designed the experiments: HK JA SO ON HY. Performed the experiments: HK JA SO SS MY MN KU KU TK KT YU ON HY. Analyzed the data: HK JA SO SS MY MN KU KU TK KT YU ON HY. Contributed reagents/materials/analysis tools: HK JA SO SS MY MN KU KU TK KT YU ON HY. Wrote the manuscript: HK JA SO ON HY.

References

1. Pestka S, Langer JA, Zoon KC, Samuel CE (1987) Interferons and their actions. Annu Rev Biochem 56: 727–777. doi:10.1146/annurev.bi.56.070187.003455. PubMed: 2441659.
2. Jonasch E, Haluska FG (2001) Interferon in oncological practice: review of interferon biology, clinical applications, and toxicities. Oncologist 6: 34–55. doi:10.1634/theoncologist.6-1-34. PubMed: 11161227.
3. Lai CL, Lau JY, Wu PC, Ngan H, Chung HT et al. (1993) Recombinant interferon-alpha in inoperable hepatocellular carcinoma: a randomized controlled trial. Hepatology. 17: 389-394. doi:10.1002/hep.1840170307. PubMed: 8383088.
4. Sakaguchi Y, Kudo M, Fukunaga T, Minami Y, Chung H et al. (2005) Low-dose, long-term, intermittent interferon-alpha-2b therapy after radical treatment by radiofrequency ablation delays clinical recurrence in patients with hepatitis C virus-related hepatocellular carcinoma. Intervirology 48: 64–70. doi:10.1159/000082097. PubMed: 15785092.
5. Miyake Y, Kobashi H, Yamamoto K (2009) Meta-analysis: the effect of interferon on development of hepatocellular carcinoma in patients with chronic hepatitis B virus infection. J Gastroenterol 44: 470–475. doi: 10.1007/s00535-009-0024-z. PubMed: 19308310.
6. Miyake Y, Iwasaki Y, Yamamoto K (2010) Meta-analysis: reduced incidence of hepatocellular carcinoma in patients not responding to interferon therapy of chronic hepatitis C. Int J Cancer 127: 989–996. PubMed: 19957327.
7. Qu LS, Jin F, Huang XW, Shen XZ (2010) Interferon-α therapy after curative resection prevents early recurrence and improves survival in patients with hepatitis B virus-related hepatocellular carcinoma. J Surg Oncol 102: 796–801. doi:10.1002/jso.21741. PubMed: 20886584.
8. Manns MP, McHutchison JG, Gordon SC, Rustgi VK, Shiffman M et al. (2001) Peginterferon alfa-2b plus ribavirin compared with interferon alfa-2b plus ribavirin for initial treatment of chronic hepatitis C: a randomised trial. Lancet 358: 958–965. doi:10.1016/S0140-6736(01)06102-5. PubMed: 11583749.
9. Fried MW, Shiffman ML, Reddy KR, Smith C, Marinos G et al. (2002) Peginterferon alfa-2a plus ribavirin for chronic hepatitis C virus infection. N Engl J Med 347: 975–982. doi:10.1056/NEJMoa020047. PubMed: 12324553.
10. Yano H, Ogasawara S, Momosaki S, Akiba J, Kojiro S et al. (2006) Growth inhibitory effects of pegylated IFN alpha-2b on human liver cancer cells *in vitro* and *in vivo*. Liver Int 26: 964–975. doi:10.1111/j.1478-3231.2006.01321.x. PubMed: 16953837.
11. Utsunomiya I, Iemura A, Yano H, Akiba J, Kojiro M (1999) Establishment and characterization of a new human hepatocellular carcinoma cell line, HAK-3, and its response to growth factors. Int J Oncol 15: 669–675. PubMed: 10493947.
12. Murakami T (1984) Establishment and characterization of human hepatoma cell line (KIM-1). Acta Hepatol Jpn 25: 532–539. doi: 10.2957/kanzo.25.532.
13. Murakami T, Maruiwa M, Fukuda K, Kojiro M, Tanaka M, et al. (1988) Characterization of a new human hepatoma cell line (KYN-3) derived from the ascites of the hepatoma patient [Abstract]. Jpn J Cancer Res 292 Proceedings of the Japanese Cancer Association
14. Murakami T, Yano H, Maruiwa M, Sugihara S, Kojiro M (1987) Establishment and characterization of a human combined hepatocholangiocarcinoma cell line and its heterologous transplantation in nude mice. Hepatology 7: 551–556. doi:10.1002/hep.1840070322. PubMed: 3032760.
15. Haramaki M, Yano H, Iemura A, Momosaki S, Ogasawara S et al. (1997) A new human hepatocellular carcinoma cell line (HAK-2) forms various structures in collagen gel matrices. Hum Cell 10: 183–192. PubMed: 9436038.
16. Yano H, Iemura A, Fukuda K, Mizoguchi A, Haramaki M et al. (1993) Establishment of two distinct human hepatocellular carcinoma cell lines from a single nodule showing clonal dedifferentiation of cancer cells. Hepatology 18: 320–327. doi:10.1016/0270-9139(93)92802-7. PubMed: 8393423.
17. Yano H, Iemura A, Haramaki M, Momosaki S, Ogasawara S et al. (1996) A human combined hepatocellular and cholangiocarcinoma cell line (KMCH-2) that shows the features of hepatocellular carcinoma or cholangiocarcinoma under different growth conditions. J Hepatol 24: 413–422. doi:10.1016/S0168-8278(96)80161-9. PubMed: 8738727.
18. Yano H, Iemura A, Haramaki M, Ogasawara S, Takayama A et al. (1999) Interferon alfa receptor expression and growth inhibition by interferon alfa in human liver cancer cell lines. Hepatology 29: 1708–1717. doi:10.1002/hep.510290624. PubMed: 10347112.
19. Yano H, Kojiro M, Nakashima T (1986) A new human hepatocellular carcinoma cell line (KYN-1) with a transformation to adenocarcinoma. In Vitro Cell Dev Biol 22: 637–646. doi:10.1007/BF02623477. PubMed: 2430933.
20. Yano H, Maruiwa M, Murakami T, Fukuda K, Ito Y et al. (1988) A new human pleomorphic hepatocellular carcinoma cell line, KYN-2. Acta Pathol Jpn 38: 953–966. PubMed: 2847482.
21. Hisaka T, Yano H, Ogasawara S, Momosaki S, Nishida N et al. (2004) Interferon-αCon1 suppresses proliferation of liver cancer cell lines *in vitro* and *in vivo*. J Hepatol 41: 782–789. doi:10.1016/j.jhep.2004.07.012. PubMed: 15519651.
22. Takemoto Y, Yano H, Momosaki S, Ogasawara S, Nishida N et al. (2004) Antiproliferative effects of interferon-alphaCon1 on ovarian clear cell adenocarcinoma *in vitro* and *in vivo*. Clin Cancer Res 10: 7418–7426. doi:10.1158/1078-0432.CCR-04-0279. PubMed: 15534119.
23. Bailon P, Palleroni A, Schaffer CA, Spence CL, Fung WJ et al. (2001) Rational design of a potent, long-lasting form of interferon: a 40 kDa branched polyethylene glycol-conjugated interferon alpha-2a for the treatment of hepatitis C. Bioconjug Chem 12: 195-202. doi:10.1021/bc000082g. PubMed: 11312680.

24. Bosman FT, Carneiro F, Hruban RH, Theise ND (2010) WHO Classification of Tumours of the Digestive System (4th Revised edition). Lyon, France, IARC Press. pp. 225-227.
25. Nagano H, Miyamoto A, Wada H, Ota H, Marubashi S et al. (2007) Interferon-alpha and 5-fluorouracil combination therapy after palliative hepatic resection in patients with advanced hepatocellular carcinoma, portal venous tumor thrombus in the major trunk, and multiple nodules. Cancer 110: 2493–2501. doi:10.1002/cncr.23033. PubMed: 17941012.
26. Gillespie G, Carter WA (1981-1982) Species specificity of interferon. Tex Rep Biol Med 41: 37-42. PubMed: 6184826.
27. Hlatky L, Hahnfeldt P, Folkman J (2002) Clinical application of antiangiogenic therapy: microvessel density, what it does and doesn't tell us. J Natl Cancer Inst 94: 883-893. doi:10.1093/jnci/94.12.883. PubMed: 12072542.
28. Kojiro S, Yano H, Ogasawara S, Momosaki S, Takemoto Y et al. (2006) Antiproliferative effects of 5-fluorouracil and interferon-alpha in combination on a hepatocellular carcinoma cell line *in vitro* and *in vivo*. J Gastroenterol Hepatol 21: 129–137. doi:10.1111/j.1440-1746.2005.04154.x. PubMed: 16706824.
29. Dinney CP, Bielenberg DR, Perrotte P, Reich R, Eve BY et al. (1998) Inhibition of basic fibroblast growth factor expression, angiogenesis, and growth of human bladder carcinoma in mice by systemic interferon-alpha administration. Cancer Res 58: 808–814. PubMed: 9485039.
30. Di Bisceglie AM, Shiffman ML, Everson GT, Lindsay KL, Everhart JE et al. (2008) Prolonged therapy of advanced chronic hepatitis C with low-dose peginterferon. N Engl J Med 359: 2429–2441. doi:10.1056/NEJMoa0707615. PubMed: 19052125.
31. Lok AS, Everhart JE, Wright EC, Di Bisceglie AM, Kim HY et al. (2011) Maintenance peginterferon therapy and other factors associated with hepatocellular carcinoma in patients with advanced hepatitis C. Gastroenterology 140: 840–849. doi:10.1053/j.gastro.2010.11.050. PubMed: 21129375.
32. Bruix J, Poynard T, Colombo M, Schiff E, Burak K et al. (2011) Maintenance therapy with peginterferon alfa-2b does not prevent hepatocellular carcinoma in cirrhotic patients with chronic hepatitis C. Gastroenterology 140: 1990–1999. doi:10.1053/j.gastro.2011.03.010. PubMed: 21419770.
33. Nishiguchi S, Tamori A, Kubo S (2005) Effect of long-term postoperative interferon therapy on intrahepatic recurrence and survival rate after resection of hepatitis C virus-related hepatocellular carcinoma. Intervirology 48: 71–75. doi:10.1159/000082098. PubMed: 15785093.

Hepatology Research

Hepatology Research 2013 doi: 10.1111/hepr.12219

Original Article

Pathological characteristics of patients who develop hepatocellular carcinoma with negative results of both serous hepatitis B surface antigen and hepatitis C virus antibody

Reiichiro Kondo,[1,4,5] Osamu Nakashima,[6] Michio Sata,[2] Fumio Imazeki,[7] Osamu Yokosuka,[7] Ken Tanikawa,[5] Masayoshi Kage,[3,4,5] Hirohisa Yano[1] and The Liver Cancer Study Group of Kyushu

[1]Department of Pathology, [2]Division of Gastroenterology, Department of Medicine, [3]Research Center for Innovative Cancer Therapy, Kurume University School of Medicine, [4]Cancer Center, [5]Department of Diagnostic Pathology, [6]Department of Clinical Laboratory Medicine, Kurume University Hospital, Kurume, and [7]Department of Medicine and Clinical Oncology, Graduate School of Medicine, Chiba University, Chiba, Japan

Aim: We tried to characterize the pathological features of patients who developed hepatocellular carcinoma (HCC) with the negative results of both serous hepatitis B surface antigen and hepatitis C virus antibody (non-B, non-C).

Methods: In a multicenter study in Kyushu, Japan, we studied the histopathological characteristics of non-cancerous liver tissues in 129 patients (103 men and 26 women) with non-B, non-C HCC. The histological liver damage was evaluated for fibrosis (stage) and inflammation (grade) according to the Ludwig classification of chronic hepatitis. In addition, we examined the hepatitis B virus (HBV) genome in serum samples and liver tissues of 20 patients with non-B, non-C HCC.

Results: Positivity of serum hepatitis B core (HBc) antibody, alcohol abuse, diabetes and non-alcoholic steatohepatitis were present in 61 (47%), 76 (59%), 57 (44%) and eight (6%) patients, respectively. The degree of fibrosis was mild (stage 1.6 ± 1.2). The stage of patients with neither serum HBc antibody nor alcohol abuse was significantly lower than the stage of patients with HBc antibody and no alcohol abuse ($P < 0.05$). HBV genome was detected in 15 cancerous tissues (75%) and 16 non-cancerous liver tissues (80%) in 20 patients with non-B, non-C HCC. Only three of the 20 patients were positive for serum HBc antibody.

Conclusion: Non-B, non-C patients appear to develop HCC at a low stage of fibrosis. Occult hepatitis B virus infection is the major risk factor for HCC of non-B, non-C patients in Kyushu, Japan.

Key words: diabetes mellitus, hepatocellular carcinoma, large liver cell change, non-alcoholic steatohepatitis, non-B non-C, occult hepatitis B infection

INTRODUCTION

HEPATOCELLULAR CARCINOMA (HCC) is the fifth most common cancer worldwide.[1–3] HCC mostly occurs within an established background of chronic liver disease and cirrhosis. Although the risk factors for HCC, including infection with hepatitis B virus (HBV) and hepatitis C virus (HCV), are well defined,[4–6] some patients with HCC in Japan have no confirmed chronic viral hepatitis, and the percentage of these patients is reportedly much higher in Western countries.[7–9]

Hepatocellular carcinoma cases without chronic viral hepatitis include patients who suffer from other chronic liver diseases predisposing to HCC, such as alcoholic liver disease,[9] hemochromatosis,[10] Budd–Chiari syndrome[11] and non-alcoholic fatty liver disease (NAFLD)/non-alcoholic steatohepatitis (NASH).[12,13] In addition, there is a subpopulation of patients with HCC that develops from normal liver or liver tissue damaged from

Correspondence: Dr Reiichiro Kondo, Department of Pathology, Kurume University School of Medicine, 67 Asahi-machi, Kurume, Fukuoka 830-0011, Japan. Email: kondou_reiichirou@kurume-u.ac.jp
Conflict of interest: The authors declare that they have no conflict of interest.
Received 9 April 2013; revision 18 July 2013; accepted 6 August 2013.

an unknown cause at a constant rate. The incidence and risk factors for HCC in patients without chronic viral hepatitis are not yet clear.

The Liver Cancer Study Group of Kyushu (LCSK) established a working group for the multicenter study to investigate the carcinogenesis of HCC without chronic viral hepatitis. The aim of the study described in the present paper was to clarify the pathological characteristics in non-cancerous liver tissues of patients who developed HCC with the negative results of both serous hepatitis B surface (HBs) antigen and HCV antibody (non-B, non-C) to investigate the carcinogenesis of HCC without chronic viral hepatitis.

METHODS

Tissues

WE STUDIED THE histopathological characteristics of 129 patients with non-B, non-C HCC between 1996 and 2006 with the LCSK and their affiliated hospital in the northern area of Kyushu, Japan. Patients with co-existing liver disease diagnosed by clinical and histological examination, such as autoimmune hepatitis, primary biliary cirrhosis, Budd–Chiari syndrome, hemochromatosis, Wilson disease and *Schistosomiasis japonica*, were excluded. Non-cancerous liver tissues were obtained by percutaneous biopsy or surgical operation (percutaneous biopsy, 65 patients; surgical operation, 64 patients).

In addition, we investigated HBV DNA in cryopreserved serum samples, HCC tissues and non-cancerous liver tissues that were obtained from 20 patients with non-B, non-C HCC in Kurume University Hospital in the period between 1997 and 2008.

This study was performed with informed consent obtained from patients for the use of their liver tissues and serum samples in the investigation and was approved by the ethical committee of Kurume University (approval ID no. 10004).

Histopathological examination of non-cancerous liver tissues

Each tissue was fixed with 10% formalin, embedded in paraffin, cut into 5-μm sections, and then used for histological analyses. The specimens were stained with hematoxylin–eosin and examined under a light microscope.

The histological liver damage of these specimens was evaluated for fibrosis and inflammation according to the Ludwig classification of chronic hepatitis.[14] The severity of fibrosis (stage of disease) was classified as none (stage 0), mild (portal fibrosis, stage 1), moderate (periportal fibrosis, stage 2), severe (bridging fibrosis with lobar distortion, stage 3) and cirrhosis (stage 4), and the inflammatory activity (grade of disease activity) was classified as none (grade 0), minimal (grade 1), mild (grade 2), moderate (grade 3) or severe (grade 4). In addition, the pathological features of hepatocytes, such as fatty change, ballooning and large liver cell change (LCC, Fig. 1), were evaluated.

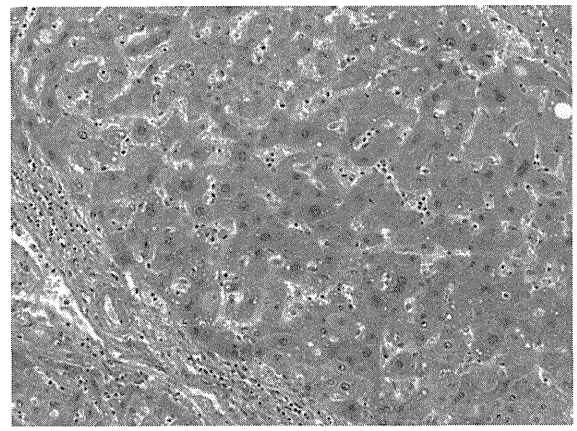

Figure 1 Microscopic findings (Large liver cell change). Large liver cell change is recognized as foci of cellular enlargement and nuclear pleomorphism, hyperchromasia and multinucleation (stained with hematoxylin and eosin, ×200).

Histopathological diagnosis and classification were performed by two pathologists (O. N. and M. K.).

Nucleic acid extraction from serum samples

Total nucleic acid was extracted from 300 μL of plasma using a commercially available kit (High Pure Viral Nucleic Acid Kit; Roche, Mannheim, Germany) according to the manufacturer's instructions. The extracted nucleic acid was eluted in 25 μL of elution buffer.

Nucleic acid extraction from liver tissues

The QIAamp DNA micro kit (QIAGEN, Hilden, Germany) was used to extract the nucleic acid from liver tissues (<10 mg) according to the manufacturer's instructions, with few changes. The DNA was eluted in 60 μL of AE buffer.

Quantification of HBV DNA (S, X, C)

Hepatitis B virus DNA was analyzed for the region of HBs, hepatitis B core (HBc), and hepatitis B x (HBx) by

Table 1 Nucleotide positions and sequences of TaqMan polymerase chain reaction primers and probes

S region	5′–3′	
Sense	TGTACAAAACCTTCGGACGGAAA	442–464
Antisense	TGCGAAAGCCCAGGATGATG	485–504
Probe	CTGCACTTGTATTCCC	465–480
Core region		
Sense	ACTGTGGTTTCACATTTCCTGTCTT	2072–2096
Antisense	GGCATTTGGTGGTCTGTAAGC	2163–2183
Probe	CCACACTCCAAAAGAC	2132–2147
X region		
Sense	CTACTGTTCAAGCCTCCAAGCT	1729–1750
Antisense	GCTCCAAATTCTTTATACGGGTCAATG	1778–1804
Probe	AAGCCACCCAAGGCAC	1751–1766

TaqMan real-time polymerase chain reaction (PCR) according to the manufacture's guidelines (Taqman Fast Universal PCR Master Mix; Applied Biosystems, Foster City, CA, USA). The oligonucleotide primers and probes that were optimized to adr of HBV subtype and specific for S, X and C region sequences, are summarized in Table 1. Plasmid pBRHBadr72 (full-length HBV DNA) was used as an internal standard in the quantitative real-time detection PCR. We used 8 μL nucleic acid from serum in our study for better sensitivity. The limit of sensitivity of our TaqMan real-time PCR methods ranged from 5 copies/well. The detection limit of our tests was 52 copies/mL. For quantification of HBV DNA from liver tissue, we used 3 μL nucleic acid, and a single copy housekeeping gene present in human, β-actin was assayed on the same sample. This was performed to estimate the number of cells presented in each PCR reaction. Serial dilutions of genomic DNA were used as standards to quantitate β-actin DNA from liver biopsies (TaqMan Beta-actin Detection Reagents; Applied Biosystems).

Enzymatic treatment with plasmid-safe adenosine triphosphate (ATP)-dependent DNase for detection of cccDNA

DNA extracted from liver tissue (<10 mg) was diluted to 60 μL in AE buffer. A 40-μL aliquot was put aside for detection of RC DNA (X, S, C regions) and β-actin DNA. The remaining 20 μL was digested with 25 units of Plasmid-Safe ATP-dependent DNase (Epicentre Technologies, Madison, WI, USA) for 30 min at 37°C in the presence of 10 × reaction buffer 5 μL, 25 mM ATP 2 μL, Plasmid-Safe DNase 1 μL and deionized distilled water 22 μL. Then, the reaction was inactivated by incubation at 70°C for 30 min. The mixture was purified using a QIAquick PCR Purification Kit (QIAGEN) and diluted by 40 μL EB buffer.

Quantification of HBV cccDNA

Hepatitis B virus cccDNA was tested using c-sel primers and probes as shown in Figure 2. We used 5 μL HBV cccDNA in the TaqMan real-time PCR. The internal standard was plasmid pBRHBadr72.

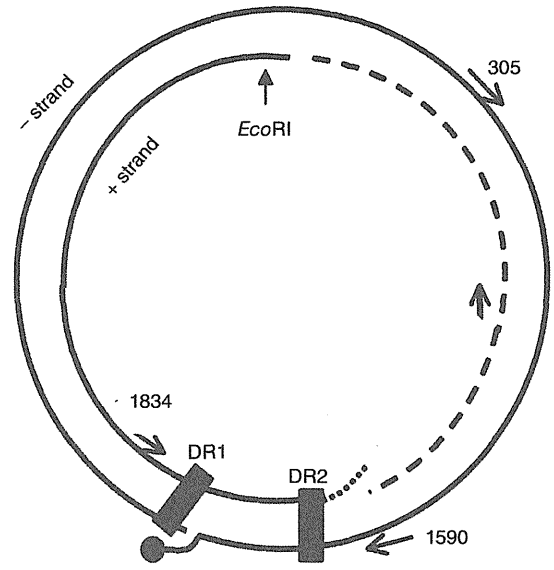

Figure 2 Quantification of HBV cccDNA. HBV cccDNA was tested using c-sel primers and probes. We used 5 μl HBV cccDNA in the Taqman real-time PCR. The internal standard was Plasmid pBRHBadr72.

Table 2 Clinical backgrounds of 129 patients examined by the LCSK

	AL (+)		AL (−)		Total
HBc (+)	40		21		61
	DM (+)	DM (−)	DM (+)	DM (−)	
	M: 15	M: 23	M: 4 (NASH: 1)	M: 8 (NASH: 1)	
	F: 1	F: 1	F: 3 (NASH: 1)	F: 6 (NASH: 1)	
	(A)	(B)	(C)	(D)	
HBc (−)	36		32		68
	DM (+)	DM (−)	DM (+)	DM (−)	
	M: 17	M: 18	M: 9	M: 9	
	F: 0	F: 1	F: 8 (NASH: 3)	F: 6 (NASH: 1)	
	(E)	(F)	(G)	(H)	
Total	76		53		129

(A) Stage 2.1 ± 1.4, grade 2.4 ± 1.2.
(B) Stage 1.8 ± 1.5, grade 1.9 ± 1.7.
(C) Stage 1.9 ± 1.1, grade 1.7 ± 1.4.
(D) Stage 1.8 ± 1.2, grade 2.2 ± 1.7.
(E) Stage 1.8 ± 1.1, grade 2.1 ± 1.2.
(F) Stage 1.3 ± 1.2, grade 1.9 ± 1.1.
(G) Stage 1.4 ± 1.3, grade 2.0 ± 1.4.
(H) Stage 1.0 ± 0.8, grade 1.4 ± 1.0.
Data are expressed as the mean ± standard deviation.
AL, alcohol abuse; DM, diabetes mellitus; F, female; HBc, serum HBc antibody; M, male; NASH, non-alcoholic steatohepatitis.

Statistical analysis

Arithmetic means and standard deviation (SD) of our data were calculated using a JMP software package (version 10.0; SAS Institute, Cary, NC, USA). All data are expressed as the mean ± SD, and *P*-values less than 5% were considered significant.

RESULTS

Clinical background

IN 129 PATIENTS with non-B, non-C HCC examined by the LCSK, there were 103 men and 26 women. The mean age of the men was 68 ± 10 years and the women 70 ± 11 years. Sixty-one patients (47%) were serum HBc antibody positive. Seventy-six patients (59%) abused alcohol (daily intake >60 g of ethanol for men, >40 g for women). Fifty-seven patients (44%) had diabetes mellitus. Most female patients (14 patients) had neither serum HBc antibody nor alcohol abuse (Table 2).

Clinical background and histological findings

Liver fibrosis and inflammation

Non-cancerous liver tissues of 129 patients with non-B, non-C HCC examined by the LCSK showed mild fibrosis and inflammation (grade 2.0 ± 1.4, stage 1.6 ± 1.2). The stage of patients with neither serum HBc antibody nor alcohol abuse was significantly lower than the stage of patients with HBc antibody and alcohol abuse (1.2 ± 1.1 vs 1.9 ± 1.4, $P < 0.03$), and the stage of patients with HBc antibody and no alcohol abuse (1.2 ± 1.1 vs 1.8 ± 1.1, $P < 0.05$) (Table 3). Patients with neither serum HBc antibody, alcohol abuse nor diabetes mellitus were of the lowest grade and stage in patients

Table 3 Clinical backgrounds and histological findings of 129 patients examined by the LCSK

	AL (+)	AL (−)	Total
HBc (+)	40	21	61
	Stage 1.9 ± 1.4	Stage 1.8 ± 1.1	
	Grade 2.1 ± 1.5	Grade 2.0 ± 1.6	
	**	*	
HBc (−)	36	32	68
	Stage 1.6 ± 1.2	Stage 1.2 ± 1.1	
	Grade 2.0 ± 1.6	Grade 1.7 ± 1.2	
Total	76	53	129

Data are expressed as the mean ± standard deviation.
*$P < 0.05$, **$P < 0.03$.
AL, alcohol abuse; HBc, serum HBc antibody; LCSK, Liver Cancer Study Group of Kyushu.

Table 4 Summary of histopathological findings in non-alcoholic patients examined by the LCSK

	Hepatic steatosis	Hepatocellular ballooning	Mallory–Denk body	Lipogranuloma	NASH
HBc (−), DM (−), $n = 15$	6	2	1	1	1
HBc (+), DM (−), $n = 14$	4	5	2	1	2
HBc (−), DM (+), $n = 17$	12	4	3	3	3
HBc (+), DM (+), $n = 7$	6	4	1	2	2

DM, diabetes mellitus; HBc, serum HBc antibody; LCSK, Liver Cancer Study Group of Kyushu; NASH, non-alcoholic steatohepatitis.

examined by the LCSK (stage 1.0 ± 0.8, grade 1.4 ± 1.0; Table 2).

Pathological features of hepatocytes

Non-cancerous liver tissues of 129 patients with non-B, non-C HCC examined by the LCSK showed various pathological features. In 53 patients without alcohol abuse, eight patients were identified as having NASH. There were six female patients of the eight patients with NASH (Table 2). NAFLD was present in 28 patients of the 53 non-alcoholic patients. Of 28 patients with NAFLD, diabetes mellitus was present in 18 (64%) patients (Table 4). LCC was observed in 52 of the 61 patients (85%) with serum HBc antibody, and 44 of the 68 patients (65%) without serum HBc antibody (Fig. 3).

HBV DNA in serum samples and liver tissues

In cryopreserved serum samples, HCC tissues and non-cancerous liver tissues obtained from 20 patients with non-B, non-C HCC, HBV DNA was detected in one serum sample (5%), 15 HCC tissues (75%) and 16 non-cancerous liver tissues (80%) (Table 5). In only two patients, both HCC tissues and non-cancerous liver tissues were negative for HBV DNA detection. In addition, only three of the 20 patients were positive for serum HBc antibody.

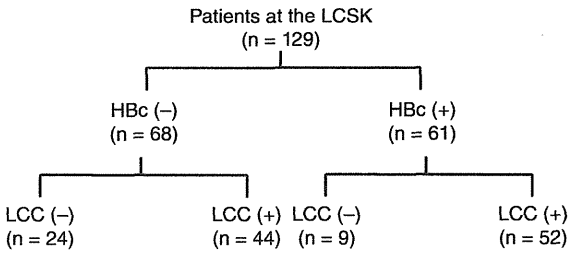

Figure 3 Large liver cell change of 129 patients examined by the Liver Cancer Study Group of Kyushu. There are 96 patients (74%) with large liver cell change (LCC) in 129 patients with non-B, non-C hepatocellular carcinoma. Large liver cell change is observed in 52 of the 61 patients (85%) with serum hepatitis B core (HBc) antibody, and 44/68 patients (65%) without serum HBc antibody.

DISCUSSION

RECENTLY, THE AVAILABILITY of vaccines for HBV has decreased the proportion of patients with HBs antigen by preventing mother-to-infant infection.[15] Antiviral therapy in patients with HCV may prevent carcinogenesis.[16,17] The incidence of HCC associated with HBV or HCV is thus forecast to decrease in Japan, whereas HCC without hepatitis virus infection will remain.[7,18] In this study, we demonstrated the pathological characteristics in non-cancerous liver tissues of patients with non-B, non-C HCC.

Patients with non-B, non-C HCC have various clinical backgrounds, such as serum HBc antibody, alcohol abuse and diabetes mellitus. Abe *et al.*[8] reported 64 patients with non-B, non-C HCC in Tokyo, Japan. Positivity of serum HBc antibody, alcohol abuse and diabetes mellitus was present in 34 (53.1%), 46 (71.9%) and 29 (45.3%) patients, respectively. Yano *et al.*[19] reported 22 patients with non-B, non-C HCC in Saga, Kyushu, Japan. Positivity of serum HBc antibody was present in 16 (72.7%) patients. In this study, we studied 129 patients with non-B, non-C HCC in the northern area of Kyushu, Japan. Positivity of serum HBc antibody, alcohol abuse and diabetes mellitus was present in 61 (47%), 76 (59%) and 57 (44%) patients, respectively. We considered that there were regional differences with respect to the frequency of the non-B, non-C HCC development risk factors, such as positivity of serum HBc antibody, alcohol abuse and diabetes mellitus.

Hepatitis C virus infection, HBV infection, alcohol abuse and NASH are the main causes of liver fibrosis.[20] In this study, non-cancerous liver tissues of patients with neither serum HBc antibody, alcohol abuse nor

Table 5 Summary of HBV DNA in serum samples and liver tissues

Case no.	Serum samples		Liver tissues							
	HBc Ab	Surface	HCC tissues				Non-cancerous tissues			
			Surface	X	Core	cccDNA	Surface	X	Core	cccDNA
1	−	−	−	+	+	−	−	+	−	−
2	+	−	−	+	−	−	−	+	−	−
3	+	−	+	−	−	−	+	+	+	+
4	−	−	−	−	−	−	−	−	−	−
5	−	−	+	−	−	−	+	+	+	−
6	−	−	−	+	−	−	+	+	−	−
7	−	−	−	−	−	−	−	−	+	−
8	−	+	−	+	−	−	−	−	−	−
9	−	−	−	−	−	−	+	−	−	−
10	−	−	+	+	+	−	+	+	+	+
11	−	−	−	+	−	−	+	+	+	−
12	−	−	+	+	+	−	+	+	−	−
13	−	−	+	+	−	−	+	+	−	−
14	−	−	+	+	−	−	+	−	−	−
15	+	−	+	−	−	+	+	+	+	−
16	−	−	+	+	+	−	−	−	+	−
17	−	−	−	−	−	−	−	−	−	−
18	−	−	−	−	−	−	+	+	−	−
19	−	−	+	+	+	−	−	+	−	−
20	−	−	−	+	−	−	−	−	−	−

Ab, antibody; core, HBV C region; HBc, hepatitis B core; HBV, hepatitis B virus; HCC, hepatocellular carcinoma; surface, HBV S region; X, HBV X region.

diabetes mellitus showed a slight degree of fibrosis. Positivity of serum HBc, alcohol abuse and diabetes mellitus may be an additive factor for liver fibrosis.

In patients with chronic viral hepatitis, HCC mostly occurs within liver cirrhosis. Liver cirrhosis results in liver failure, portal hypertension and increased risk of carcinogenesis.[21] In this study, non-cancerous liver tissues of 129 patients with non-B, non-C HCC examined by the LCSK showed mild fibrosis and inflammation. We consider that patients without chronic viral hepatitis may have another risk factor for HCC apart from liver fibrosis.

It has been suggested that NASH may account for a substantial portion of cryptogenic HCC cases.[22] In this study, 129 patients with non-B, non-C HCC examined by the LCSK included 28 patients with NAFLD. Of these, diabetes mellitus was present in 18 (64%) patients. NAFLD has been widely accepted as a possible etiological factor in the development of non-B, non-C HCC; because of the fact that diabetes mellitus was common in patients with NAFLD, insulin resistance may further facilitate the development of HCC.

In addition, there were 96 patients (74%) with LCC of the 129 patients with non-B, non-C HCC examined by the LCSK in this study. LCC was observed in 52 of the 61 patients (85%) with serum HBc antibody, and 44 of the 68 patients (65%) without serum HBc antibody. LCC is characterized by individually scattered or clusters of hepatocytes with atypia, measuring less than 1 mm in diameter, which do not form circumscribed nodules, and have been often found in chronic liver disease.[23,24] LCC is recognized under the microscope as the foci of cellular enlargement and nuclear pleomorphism, hyperchromasia and multinucleation. Although LCC is frequently found in various liver diseases and easily recognized even under low-power magnification due to the characteristic cytological features, its pathological significance is still under debate. LCC has been reported to be observed in various liver diseases such as autoimmune hepatitis, alcoholic cirrhosis and cholestatic liver, although it is more prevalent in HBV-related chronic liver disease.[24–26] It was reported that LCC in HBV-related chronic liver disease demonstrated molecular characteristics different from that in chronic

cholestasis.[27] We also confirmed in this study that HBV DNA was detected in 15 HCC tissues (75%) and 16 non-cancerous liver tissues (80%) obtained from 20 patients with non-B, non-C HCC, although only three of the 20 patients were positive for serum HBc antibody. Based on these findings, we consider that occult HBV infection may be present in a considerable number of patients without serum HBc antibody and occult HBV infection is the major risk factor for the development of HCC in patients without chronic viral hepatitis in the northern area of Kyushu, Japan. Recently, a relationship between the incidence of non-B, non-C HCC and occult HBV infection has been reported.[28–30] The HBV genome persists in a high percentage of HBs antigen negative patients, with and without antibodies against the virus, who develop HCC.[28] It was reported that HBV DNA was detectable in a high proportion of HCC patients without HBs antigen in Japan.[29,30]

In conclusion, the results obtained in the present study indicate that non-cancerous liver tissues of patients with non-B, non-C HCC showed mild fibrosis and inflammation, although serum HBc antibody, alcohol abuse and diabetes mellitus may be additional factors for liver fibrosis. In addition, HBV DNA was detectable in a high proportion of patients with non-B, non-C HCC. Further study of the interaction between HBV DNA in liver tissues and cellular protein will contribute to understanding the involvement of HBV in the HCC of unknown etiology.

ACKNOWLEDGMENT

WE ARE INDEBTED to Dr Motoo Akaboshi, Dr Yuichi Tanabe, Dr Akinari, Tabaru, Dr Hiroshi Watanabe, Dr Akinobu Taketomi, Dr Kunitaka Fukuizumi, Dr Yuko Takami, Dr Toshihiko Mizuta, Dr Naota Taura and Dr Nobuyoshi Fukushima. We would like to thank the members of the Liver Cancer Study Group of Kyushu for their assistance in conducting the study. This study was supported in part by Health and Labour Sciences Research Grants for Research on Hepatitis from the Ministry of Health, Labour and Welfare of Japan.

REFERENCES

1 Parkin DM. Global cancer statistics in the year 2000. *Lancet Oncol* 2001; **2**: 533–43.
2 El-Serag HB, Marrero JA, Rudolph L, Reddy KR. Diagnosis and treatment of hepatocellular carcinoma. *Gastroenterology* 2008; **134**: 1752–63.
3 Starley BQ, Calcagno CJ, Harrison SA. Nonalcoholic fatty liver disease and hepatocellular carcinoma: a weighty connection. *Hepatology* 2010; **51**: 1820–32.
4 Di Bisceglie AM, Goodman ZD, Ishak KG, Hoofnagle JH, Melpolder JJ, Alter HJ. Long-term clinical and histopathological follow-up of chronic posttransfusion hepatitis. *Hepatology* 1991; **14**: 969–74.
5 Kiyosawa K, Sodeyama T, Tanaka E *et al.* Interrelationship of blood transfusion, non-A, non-B hepatitis and hepatocellular carcinoma: analysis by detection of antibody to hepatitis C virus. *Hepatology* 1990; **12**: 671–5.
6 Davila JA, Morgan RO, Shaib Y, McGlynn KA, El-Serag HB. Hepatitis C infection and the increasing incidence of hepatocellular carcinoma: a population-based study. *Gastroenterology* 2004; **127**: 1372–80.
7 Taura N, Fukushima N, Yatsuhashi H *et al.* The incidence of hepatocellular carcinoma associated with hepatitis C infection decreased in Kyushu area. *Med Sci Monit* 2010; **17**: 7–11.
8 Abe H, Yoshizawa K, Kitahara T, Aizawa R, Matsuoka M, Aizawa Y. Etiology of non-B non-C hepatocellular carcinoma in the eastern district of Tokyo. *J Gastroenterol* 2008; **43**: 967–74.
9 Seeff LB, Hoofnagle JH. Epidemiology of hepatocellular carcinoma in areas of low hepatitis B and hepatitis C endemicity. *Oncogene* 2006; **25**: 3771–7.
10 Haddow JE, Palomaki GE, McClain M, Craig W. Hereditary haemochromatosis and hepatocellular carcinoma in males: a strategy for estimating the potential for primary prevention. *J Med Screen* 2003; **10**: 11–3.
11 Moucari R, Rautou PE, Cazals-Hatem D *et al.* Hepatocellular carcinoma in Budd-Chiari syndrome: characteristics and risk factors. *Gut* 2008; **57**: 828–35.
12 Marrero JA, Fontana RJ, Su GL, Conjeevaram HS, Emick DM, Lok AS. NAFLD may be a common underlying liver disease in patients with hepatocellular carcinoma in the United States. *Hepatology* 2002; **36**: 1349–54.
13 Yasui K, Hasimoto E, Komorizono Y *et al.* Charactaristics of patients with nonalcoholic steatohepatitis who develop hepatocellular carcinoma. *Clin Gastroenterol Hepatol* 2011; **9**: 428–33.
14 Ludwig J. The nomenclature of chronic active hepatitis: an obituary. *Gastroenterology* 1993; **105**: 274–8.
15 Chang MH, Chen CJ, Lai MS *et al.* Universal hepatitis B vaccination in Taiwan and the incidence of hepatocellular carcinoma in children. *N Engl J Med* 1997; **336**: 1855–9.
16 Nishiguchi S, Kuroki T, Nakatani S *et al.* Randomized trial of effects of interferon-alpha on incidence of hepatocellular carcinoma in chronic active hepatitis C with cirrhosis. *Lancet* 1995; **346**: 1051–5.
17 Nishiguchi S, Tamori A, Kudo S. Effects of long-term postoperative interferon therapy on intrahepatic recurrence and survival rate after resection of hepatitis C virus-related hepatocellular carcinoma. *Intervirology* 2005; **48**: 71–5.

18 Kawaguchi T, Kakuma T, Yatsuhashi H *et al.* Date mining reveals complex interactions of risk factors and clinical feature profiling associated with the staging of non-hepatitis B virus/non-hepatitis C virus-related hepatocellilar carcinoma. *Hepatol Res* 2011; **41**: 564–71.
19 Yano Y, Yamashita F, Sumie S *et al.* Clinical features of hepatocellular carcinoma seronegative for both HBsAg and anti-HCV antiboby but positive for anti-HBc antibody in Japan. *Am J Gastroenterol* 2002; **97**: 156–61.
20 Friedman SL. Liver fibrosis-from bench to bedside. *J Hepatol* 2003; **38** (Suppl 1): S38–53.
21 Bataller R, Brenner DA. Liver fibrosis. *J Clin Invest* 2005; **115**: 209–18.
22 El-Serag HB, Rudolph KL. Hepatocellular carcinoma: epidemiology and molecular carcinogenesis. *Gastroenterology* 2007; **132**: 2557–76.
23 Crawford JM. Pathological assessment of liver cell dysplasia and benign liver tumors: differentiation from malignant tumors. *Semin Diagn Pathol* 1990; **7**: 115–28.
24 Park YN, Roncalli M. Large liver cell dysplasia: a controversial entity. *J Hepatol* 2006; **45**: 734–43.
25 Paradis V, Laurendeau I, Vidaud M, Bedossa P. Clonal analysis of macronodules in cirrhosis. *Hepatology* 1998; **28**: 953–8.
26 Libbrecht L, Craninx M, Nevens F, Desmet V, Roskams T. Predictive value of liver cell dysplasia for development of hepatocellular carcinoma in patients with non-cirrhotic and cirrhotic chronic viral hepatitis. *Histopathology* 2001; **39**: 66–73.
27 Kim H, Oh BK, Roncalli M *et al.* Large liver cell change in hepatitis B virus-related liver cirrhosis. *Hepatology* 2009; **50**: 752–62.
28 Feitelson MA, Duan LX. Hepatitis B virus x antigen in the pathogenesis of chronic infections and the development of hepatocellular carcinoma. *Am J Pathol* 1997; **150**: 1141–57.
29 Shiota G, Oyama K, Udagawa A *et al.* Occult hepatitis B virus infection in HBs antigen-negative hepatocellular carcinoma in a Japanese population: involvement of HBx and p53. *J Med Virol* 2000; **61**: 151–8.
30 Tamori A, Nishiguchi S, Kudo S *et al.* HBV DNA integration and HBV-transcript expression in non-B, non-C hepatocellular carcinoma in Japan. *J Med Virol* 2003; **71**: 492–8.

Clinicopathologic Analysis of Combined Hepatocellular-Cholangiocarcinoma According to the Latest WHO Classification

Jun Akiba, MD, PhD, Osamu Nakashima, MD, PhD,† Satoshi Hattori, PhD,‡ Ken Tanikawa, MD, PhD,* Miki Takenaka, MD,* Masamich Nakayama, MD,* Reiichiro Kondo, MD,* Yoriko Nomura, MD,* Keiko Koura, MD,* Kousuke Ueda, MD,* Sakiko Sanada, MD, PhD,* Yoshiki Naito, MD, PhD,* Rin Yamaguchi, MD, PhD,* and Hirohisa Yano, MD, PhD**

Abstract: Combined hepatocellular-cholangiocarcinoma comprises < 1% of all liver carcinomas. The histogenesis of combined hepatocellular-cholangiocarcinoma has remained unclear for many years. However, recent advances in hepatic progenitor cell (HPC) investigations have provided new insights. The concept that combined hepatocellular-cholangiocarcinoma originates from HPCs is adopted in the chapter "combined hepatocellular-cholangiocarcinoma" of the latest World Health Organization (WHO) classification. In this study, we conducted clinicopathologic analysis of combined hepatocellular-cholangiocarcinoma according to the latest WHO classification. Fifty-four cases were included in this study. Pathologic diagnosis was made according to the WHO classification. When a tumor contained plural histologic patterns, predominant histologic pattern (≥ 50%) was defined. Minor histologic patterns were also appended. Immunohistochemical staining with biliary markers (CK7, CK19, and EMA), hepatocyte paraffin (HepPar)-1, HPC markers (CD56, c-kit, CD133, and EpCAM), and vimentin was performed. Forty-five and 50 patients were analyzed for progression-free survival and overall survival, respectively. Ten, 1, 32, and 11 cases were diagnosed as: combined hepatocellular-cholangiocarcinoma, classical type; combined hepatocellular-cholangiocarcinoma, stem cell features, typical subtype; combined hepatocellular-cholangiocarcinoma, stem cell features, intermediate cell subtype; and combined hepatocellular-cholangiocarcinoma, stem cell features, cholangiolocellular type, respectively. Combined hepatocellular-cholangiocarcinomas usually have high expression of biliary markers. CD56, c-kit, and EpCAM were expressed to various degrees in all combined hepatocellular-cholangiocarcinomas apart from the hepatocellular carcinoma component of combined hepatocellular-cholangiocarcinoma, classical type. The expression of CD133 and vimentin was observed only in combined hepatocellular-cholangiocarcinoma, stem cell features of intermediate cell subtype and cholangiolocellular subtype. The expression of CD133, EpCAM, and vimentin was significantly high in combined hepatocellular-cholangiocarcinoma, subtypes with stem cell features, especially cholangiolocellular subtype. Minor histologic patterns were significantly frequent in combined hepatocellular-cholangiocarcinoma, subtypes with stem cell features, compared with combined hepatocellular-cholangiocarcinoma, classical type. There was no significant difference in clinical outcome between each subtype. Combined hepatocellular-cholangiocarcinoma has wide histologic diversity and shows immunophenotypic expression of not only biliary markers but also HPC markers to various degrees, suggesting that the histogenesis of combined hepatocellular-cholangiocarcinoma could be strongly associated with HPCs. Our results pathologically validate the latest WHO classification of combined hepatocellular-cholangiocarcinoma. However, the complex mixture of histologic subtypes has presented a challenge to the classification of combined hepatocellular-cholangiocarcinoma. Further study should be conducted using a large cohort to support this classification.

Key Words: combined hepatocellular-cholangiocarcinoma, WHO classification, immunohistochemical stain

(*Am J Surg Pathol* 2013;37:496–505)

From the *Department of Pathology, Kurume University School of Medicine; †Department of Clinical Laboratory Medicine, Kurume University Hospital; and ‡Biostatistics Center, Kurume University, Kurume, Japan.

Conflicts of Interest and Source of Funding: O.N. is supported, in part, by The Vehicle Racing Commemorative Foundation. For the remaining authors none were declared.

Correspondence: Jun Akiba, MD, PhD, Department of Pathology, Kurume University School of Medicine, 67 Asahimachi, Kurume 830-0011, Japan (e-mail: akiba@med.kurume-u.ac.jp).

With the recent advances in molecular biology, cancer stem cell theory has been widely accepted in not only hematopoietic neoplasms but also solid neoplasms.[1–3] Cancer stem cells are generally defined on the basis of 4 criteria: high efficiency self-renewal, differentiation along at least 2 independent lineages, resistance to conventional genotoxic therapy, and capacity to establish and recapitulate the original tumor.[4] Liver cancers, including hepatocellular carcinoma (HCC), combined

hepatocellular-cholangiocarcinoma, and cholangiocellular carcinoma, are thought to originate from hepatic progenitor cells (HPCs; also referred to as oval cells, tumor-initiating stem-like cells).[5–8] HPCs are liver-specific adult stem cells that are activated when mature hepatocytes and/or cholangiocytes are damaged. HPCs have bipotential: they are capable of differentiation into either hepatocytes or cholangiocytes.[9–11] Although no markers for putative HPCs have yet been generally accepted, CD133, CD90, CD44, epithelial cell adhesion molecule (EpCAM), OV6, CD13, and c-kit are thought to be candidates for HPC markers.[12–23]

The vast majority of malignant primary liver cancer is HCC. Combined hepatocellular-cholangiocarcinoma is relatively rare, comprising <1% of all liver carcinomas.[24] The concept that combined hepatocellular-cholangiocarcinoma originates from HPCs is adopted in the chapter "combined hepatocellular-cholangiocarcinoma" of the latest World Health Organization (WHO) classification of the digestive system. According to the WHO classification, combined hepatocellular-cholangiocarcinoma is divided into classical type and subtypes with stem cell features. Moreover, the latter is subdivided into typical subtype, intermediate cell subtype, and cholangiolocellular subtype. The histologic features of each subtype are shown in Table 1. In our present study, we reassessed 54 cases previously diagnosed as combined hepatocellular-cholangiocarcinoma or cholangiolocellular carcinoma according to the latest WHO classification, by morphologic observation and using immunohistochemical (IHC) stains of hepatocellular, biliary/HPC markers and vimentin.

MATERIALS AND METHODS

Patients

Fifty-four cases previously diagnosed as combined hepatocellular-cholangiocarcinoma or cholangiolocellular carcinoma were reevaluated in this study. For diagnosis, we used the classification by Goodman et al[25] and Kim et al[26] for combined hepatocellular-cholangiocarcinoma and that by Stainer et al[27] for cholangiolocellular carcinoma. All cases were resected at Kurume University Hospital between 1993 and 2010. Two previously reported cases were included in this study.[6,9] Liver specimens were fixed in 10% buffered formalin, followed by paraffin embedment. We cut consecutive 4-μm-thick sections and stained them with hematoxylin and eosin and mucicarmine.

Pathologic diagnosis was performed according to the 2010 WHO classification as described before. When a tumor contained plural histologic patterns, predominant histologic pattern (≥ 50%) was defined. Minor histologic components were also appended. All slides were evaluated by 2 pathologists (J.A. and O.N.). Clinical follow-up data were available for progression-free survival (PFS) (554 ± 814 d) in 45 patients and overall survival (OS) (757 ± 828 d) in 50 patients.

This study was approved by the ethical committee of Kurume University (approved #10294).

IHC Stain

We performed IHC analysis on paraffin-embedded sections using the following antibodies: cytokeratin (CK) 7 (OV-TL 12/30; Dako, Glostrup, Denmark), CK19 (BA1; Dako), epithelial membrane antigen (EMA) (E29; Dako), hepatocyte paraffin (HepPar)-1 (OCH1E5; Dako), CD56 (1B6; Novocastra, Newcastle, UK), c-kit (K963; IBL, Fujioka, Japan), CD133 (AC133, Mileni Biotec, Auburn, CA), EpCAM (HEA125, abcam, Cambridge, UK), and vimentin (V-9; Immunon, Pittsburgh, PA). IHC staining was performed using the streptavidin-biotin-peroxidase method. Immunoreactivity was evaluated with grading from 0 to 4 as follows according to the distribution area of positive cells regardless of the staining intensity: 0, no staining; 1, 1% to 5% positive cells; 2, 6% to 25% positive cells; 3, 26% to 50% positive cells; and 4, >50% positive cells. Equivocal reaction was regarded as negative. The HCC component and the cholangiocarcinoma (ChC) component of combined hepatocellular-cholangiocarcinoma, classical type, were evaluated separately.

TABLE 1. Histologic Features of Combined Hepatocellular-Cholangiocarcinomas According to WHO Classification

Subtypes	Mucin Production	Stroma	Histologic Findings
CHC-classical			
HCC component	None	Scarce	Typical HCC, well to poorly differentiated type
ChC component	Observed	Intermediate-abundant	Typical adenocarcinoma, well to poorly differentiated type
CHC-SC-typical	None	Abundant	Nests of mature looking hepatocytes with peripheral clusters of small cells that have a high nucleus:cytoplasm ratio and hyperchromatic nuclei
CHC-SC-int	None	Intermediate-abundant	Tumor cells show features intermediate between hepatocytes and cholangiocytes. These tumor cells show strands, solid nests and/or trabeculae of small, uniform cells with scant cytoplasm and hyperchromatc nuclei
CHC-SC-CLC	None	Abundant	Tumor is composed of admixtures of small monotonous glands, antler-like anastomosing patterns. Each tumor cell is cuboidal, smaller in size than normal hepatocytes, with high nucleus:cytoplasm ratio, and distinct nucleoli

CHC indicates combined hepatocellular-cholangiocarcinoma; CHC-SC-typical, combined hepatocellular-cholangiocarcinoma, stem cell features, typical subtype; CHC-SC-int, combined hepatocellular-cholangiocarcinoma, stem cell features, intermediate cell subtype; CHC-SC-CLC, combined hepatocellular-cholangiocarcinoma, stem cell features, cholangiolocellular subtype.

Statistical Analysis

The association between the HCC or ChC component of combined hepatocellular-cholangiocarcinoma, classical type, and combined hepatocellular-cholangiocarcinoma, subtypes with stem cell features, was examined by the Fisher exact test. PFS was defined as the period from the date of resection to that of progressive disease or death. OS was defined as the period from the date of resection to that of death due to any cause. Kaplan-Meier analysis and the log rank test were used to demonstrate and compare survival curves. Differences were considered significant at $P < 0.05$. Analysis was performed using SAS version 9.2 (SAS Institute Inc., NC) and R version 2.9.0 (R Project Team).

RESULTS

Clinicopathologic Analysis

Of 54 cases, 10, 1, 32, and 11 were diagnosed as: combined hepatocellular-cholangiocarcinoma, classical type; combined hepatocellular-cholangiocarcinoma, stem cell features, typical subtype; combined hepatocellular-cholangiocarcinoma, stem cell features, intermediate cell subtype; and combined hepatocellular-cholangiocarcinoma, stem cell features, cholangiolocellular type, respectively. Combined hepatocellular-cholangiocarcinoma, stem cell features, typical subtype, was excluded from statistical analysis because of the limited number of cases. Clinicopathologic findings of each histologic type are summarized in Table 2. There was no statistical difference in the age of the patients or tumor size among all histologic types. Men were dominant in each histologic type. Patients with hepatitis B virus (HBV) or/and hepatitis C virus (HCV) infection were frequently observed in combined hepatocellular-cholangiocarcinoma. No significant difference was found in the ratio of hepatitis virus infection among all histologic types. The ratio of cases presenting vascular invasion was not significant between combined hepatocellular-cholangiocarcinoma, classical type, and combined hepatocellular-cholangiocarcinoma, subtypes of stem cell features. The ratio of cases with minor histologic components was significantly high in combined hepatocellular-cholangiocarcinoma, subtypes with stem cell features, compared with combined hepatocellular-cholangiocarcinoma, classical type ($P < 0.01$).

Histologic and IHC Findings

Representative morphologic and IHC features of each histologic type are described in Figures 1A–D. Comparisons of IHC scores among HCC or ChC components of combined hepatocellular-cholangiocarcinoma, classical type, combined hepatocellular-cholangiocarcinoma, stem cell features, intermediate cell subtype, and combined hepatocellular-cholangiocarcinoma, stem cell features, cholangiolocellular subtype, are shown in Tables 3–5. Combined hepatocellular-cholangiocarcinoma, stem cell features, typical subtype, was excluded from statistical analysis because of the limited number of cases. The HCC component of combined hepatocellular-cholangiocarcinoma, classical type, had significantly higher expression of HerPar-1 compared with that of combined hepatocellular-cholangiocarcinoma, subtypes with stem cell features. In contrast, this component had statistically lower expression compared with the others, apart from c-kit (Table 3). The IHC score of CD133, EpCAM, and vimentin in combined

TABLE 2. Clinicopathologic Findings of Each Histologic Type of Combined Hepatocellular-Cholangiocarcinomas

	CHC-classical	CHC-SC-typical	CHC-SC-int	CHC-SC-CLC
Number	10	1	32	11
Age	67.6 ± 11.0	57	65.3 ± 10.8	67.8 ± 8.3
Sex (M/F)	9/1	0/1	27/5	9/2
Etiology				
NBNC	2	1	9	8
HBV	3	0	9	2
HCV	6	0	14	1
Background liver tissue				
Chronic hepatitis	9	1	18	10
Liver cirrhosis	1	—	13	—
Others	—	—	1	1
Tumor size (mm)	45.6 ± 35.3	30	41.2 ± 23.5	38.3 ± 17.0
Vascular invasion				
Portal vein	9	1	22	6
Hepatic vein	0	0	2	2
Minor component				
HCC-like	—	1	15	5
ChC	—	1	6	1
int-like	1	—	—	—
CLC-like	1	—	1	—

One patient with coinfection of HBV and HCV was included in CHC-classical.
The ratio of cases presenting vascular invasion was not significant between CHC-classical and CHC-SC subtypes (χ^2 test: NS).
The ratio of the cases with minor components was significantly high in CHC-SC subtypes compared with CHC-classical (χ^2 test: $P < 0.01$).
CHC-classical indicates combined hepatocellular-cholangiocarcinoma, classical type; CHC-SC-typical, combined hepatocellular-cholangiocarcinoma, stem cell features, typical subtype; CHC-SC-int, combined hepatocellular-cholangiocarcinoma, stem cell features, intermediate cell subtype; CHC-SC-CLC, combined hepatocellular-cholangiocarcinoma, stem cell features, cholangiolocellular subtype; NBNC, non-HBV non-HCV.